Journal of Hazardous Materials 184 (2010) 515–522

Contents lists available at ScienceDirect

Journal of Hazardous Materials

journal homepage: www.elsevier.com/locate/jhazmat

# Preparation of iron-impregnated granular activated carbon for arsenic removal from drinking water

Qigang Chang[a,b], Wei Lin[a,*], Wei-chi Ying[b]

[a] Department of Civil Engineering, North Dakota State University, Fargo, ND 58105, USA
[b] School of Resource and Environmental Engineering, East China University of Science and Technology, Shanghai 200237, China

ARTICLE INFO

*Article history:*
Received 22 June 2010
Received in revised form 16 August 2010
Accepted 19 August 2010
Available online 26 August 2010

*Keywords:*
Arsenic
Iron impregnation
Activated carbon
Drinking water

ABSTRACT

Granular activated carbon (GAC) was impregnated with iron through a new multi-step procedure using ferrous chloride as the precursor for removing arsenic from drinking water. Scanning electron microscopy (SEM) and energy dispersive X-ray spectroscopy (EDS) analysis demonstrated that the impregnated iron was distributed evenly on the internal surface of the GAC. Impregnated iron formed nano-size particles, and existed in both crystalline (akaganeite) and amorphous iron forms. Iron-impregnated GACs (Fe-GACs) were treated with sodium hydroxide to stabilize iron in GAC and impregnated iron was found very stable at the common pH range in water treatments. Synthetic arsenate-contaminated drinking water was used in isotherm tests to evaluate arsenic adsorption capacities and iron use efficiencies of Fe-GACs with iron contents ranging from 1.64% to 12.13% (by weight). Nonlinear regression was used to obtain unbiased estimates of Langmuir model parameters. The arsenic adsorption capacity of Fe-GAC increased significantly with impregnated iron up to 4.22% and then decreased with more impregnated iron. Fe-GACs synthesized in this study exhibited higher affinity for arsenate as compared with references in literature and shows great potential for real implementations.



## 1. Introduction

Arsenic in drinking water is a great concern because long-term exposure to arsenic-contaminated drinking water can cause skin, kidney, lung, and bladder cancers [1]. Arsenic is introduced into the environment through a combination of natural processes and anthropogenic activities [2]. Soil leaching is the primary contributor of dissolved arsenic in groundwater [3]. The occurrence of arsenic in natural water is a worldwide problem and impacts a large population of human beings [4–7]. In 2001, the United States Environmental Protection Agency (USEPA) adopted a new drinking water arsenic standard of 10 μg/L, downward from the old standard of 50 μg/L [8]. This new arsenic standard presented a big challenge to existing water treatment facilities for compliance.

Technologies, including precipitation/coprecipitation, ion exchange, membrane filtration, and adsorption, have been developed to remove arsenic from drinking water [9–17]. Activated carbon is widely used to control odor/taste and remove contaminants in water treatment processes because of its huge specific surface area and well-developed pore structures [18]. Research found that arsenic adsorption capacity increased significantly after activated carbon was impregnated with iron and GAC still remained its capability to remove organic contaminants [19–28].

Different methods have been developed to impregnate GAC with more iron so as to increase arsenic adsorption capacity. A simple method was to use ferric solution as the precursor and precipitate ferric onto GAC with pH adjustment [22,24,26,29]. High amount of iron on GAC, as high as 33.6%, was achieved using this method [24]. However, the impregnated iron mainly deposited on the exterior surface of GAC rather the internal surface because ferric precipitates were too large to diffuse into pores of GAC [23]. The primary advantage of using GAC because of its large specific surface over other materials was not properly used [24,29]. In addition, iron impregnated on the exterior surface was susceptible to stability issue and lost adsorption capacity in column operations [24,30].

Arsenic adsorption on iron is a surface reaction in which arsenic forms inner-sphere surface complexation with iron [31–35]. Total surface area of impregnated iron determines the maximum arsenic adsorption capacity rather than iron amount alone. To achieve a better iron distribution inside GAC, another method was proposed to use ferrous as the precursor and followed by an in situ oxidation of ferrous to ferric [23,27]. This approach was able to impregnate iron inside GAC; however, when the iron content was 7% or higher, a concentrated iron ring was formed on the outside of GAC particles [23]. To date, it remains a challenge to impregnate GAC with a high amount of iron that is stably and evenly distributed inside GAC.

* Corresponding author. Tel.: +1 701 231 6288; fax: +1 701 231 6185.
*E-mail address:* wei.lin@ndsu.edu (W. Lin).

0304-3894/$ – see front matter © 2010 Elsevier B.V. All rights reserved.
doi:10.1016/j.jhazmat.2010.08.066

**Table 1**
The properties of GACs used in this study.

| GAC | BET specific surface area ($m^2/g$) | Total pore volume ($cm^3/g$) | Particle size (mm) |
|---|---|---|---|
| Darco 20 × 50 | 650 | 0.950 | 0.3–0.85 |
| Norit RX3 EXTRA | 1316 | 0.694 | 3.0 |

In addition, as most research focused on the development of impregnation methods, there is a lack of understandings on how the characteristics of iron, such as amount, morphology, distribution, and species, affect the arsenic adsorption behavior on iron-impregnated GAC (Fe-GAC).

The objectives of this study were to: (1) develop a method to impregnate GAC with a high amount of iron that is stably and evenly distributed in GAC; (2) characterize Fe-GAC to determine the amount, distribution, morphology, and species of impregnated iron; and (3) investigate impacts of the amount of impregnated iron on arsenic adsorption capacity and efficiency.

## 2. Experimental

### 2.1. Materials

Two commercial GACs, Darco 20 × 50 and Norit RX3 EXTRA (Table 1), were used in this study. Darco 20 × 50 is a macro-pore GAC that has a relatively small specific surface area while a large pore volume. Darco 20 × 50 was found very suitable for iron impregnation [23]. Norit RX3 EXTRA is an extruded pellet-shaped GAC with excellent mechanical strength. Unlike Darco 20 × 50, Norit RX3 EXTRA is a micro-pore GAC that has a high specific surface area while a small pore volume. GACs were thoroughly washed using de-ionized (DI) water to clean impurities and powder, dried at 105 °C overnight, and stored in desiccator.

All chemicals used in this study, including ferrous chloride, sodium arsenate, hydrochloric acid, nitric acid, sodium hydroxide, and sodium bicarbonate, were of reagent grade. Synthetic arsenate-contaminated drinking water was prepared with sodium arsenate in DI-water.

### 2.2. Preparation of Fe-GAC

A multi-step procedure was developed to impregnate GAC with iron to achieve high amounts, even distribution, and stability of iron. Ferrous chloride was used as the precursor due to its high solubility at a wide pH range. Thirty grams of GAC was added into a 250-mL glass bottle filled with 0.5 M ferrous chloride solution without headspace to prevent ferrous oxidation and precipitation. The bottle was placed on a rotating shaker for 24 h at room temperature to achieve fully penetration and saturation of ferrous in GAC pores. Then, the GAC was separated from the ferrous solution and placed in a convective oven at 105 °C for 10 h. In the oven, ferrous was oxidized to ferric making it less soluble at the same time when GAC was dried. Above steps were repeated several times resulting in more impregnated iron after each repetition.

At the end of the synthesis, a post-treatment was conducted in which Fe-GAC reacted with 1 N NaOH for 24 h. Then, the Fe-GAC was soaked in a diluted HCl solution for 24 h to remove hydroxide residue. The Fe-GAC was washed thoroughly using DI-water and dried at 105 °C. The Fe-GAC used in isotherm tests was post-treated unless specifically stated.

### 2.3. Characterization of Fe-GAC

Fe-GACs were evaluated based on four indicators: amount of impregnated iron, distribution of impregnated iron, stability of impregnated iron, and arsenate adsorption capacity of Fe-GAC. Iron content (defined in Eq. (1)) was determined through an acid extraction method. Distribution and morphology of impregnated iron were measured by scanning electron microscopy (SEM) and energy dispersive X-ray spectroscopy (EDS). Iron species were identified by X-ray diffraction (XRD). According to the objectives of this study, the pore structure and surface chemistry of Fe-GACs were not investigated.

$$\text{Iron content} = \frac{\text{mass of iron}}{\text{mass of GAC} + \text{mass of iron}} \times 100\% \quad (1)$$

#### 2.3.1. Measurement of iron content

Three different methods, incineration [36], incineration and digestion [24], and acid extraction [37], were evaluated for the measurement of the amount of impregnated iron in GAC. The acid extraction method was selected and modified for this study. Three hundred milligrams of Fe-GAC was added into a 40-mL vial containing 30 mL 1:1 HCl solution and shaken for 10 h. Then, the vial was placed in a water bath at 70–80 °C for 4 h. The Fe-GAC was separated from the solution using GF/C filter paper. The iron concentration in the filtrate was analyzed using the phenanthroline method with a Hach spectrophotometer DR5000. The iron content was calculated according to the Eq. (1).

#### 2.3.2. Measurement of the distribution, morphology, and species of impregnated iron

Fe-GACs were fractured to expose the internal structure for the examination of the distribution and morphology of impregnated iron using a JEOL JSM-6490LV scanning electron microscope equipped with a Thermo Energy Dispersive X-ray System. To avoid the destruction of the surface characteristics of Fe-GACs, no further polishing action was conducted on exposed cross-sections.

XRD analysis was carried out to determine iron species in GACs using a Bruker AXS' D8 Discover diffractometer in Bragg–Brentano geometry, using Cu Kα radiation with a wavelength of 1.5406 nm. The powdered samples of Fe-GACs were scanned from 5° to 85°, using a step size of 0.02° and a run time of 1 s/step.

### 2.4. Iron desorption test

This test was conducted to evaluate the stability of impregnated iron. Five hundred milligrams of Fe-GAC was added to 40 mL DI-water and shaken 48 h. Fe-GACs were separated through filtration using GF/C filter paper. The iron concentration in the filtrate was analyzed using the same method described in Section 2.3.1. Desorption of impregnated iron was evaluated according to the mass of dissolved iron in DI-water.

### 2.5. Arsenic adsorption test

The arsenic adsorption capacities of Fe-GACs were evaluated in batch experiments using arsenate as adsorbate. An arsenate stock solution with $As^{5+}$ concentration of 1000 mg/L was prepared using $Na_2HAsO_4$. An arsenate working solution of 40 mg/L was prepared freshly for each experiment. A constant dosage of Fe-GAC was used while the initial arsenate concentration varied. One hundred milligrams of Fe-GAC was added into a 40-mL glass vial containing 35 mL arsenate solutions. The vials were placed on the rotating shaker for 48 h at 30 rpm and 25 °C. To keep conditions close to those of natural water, pH was controlled around 7.0 using a 0.05 N $NaHCO_3$ buffer solution. After mixing, GAC was separated from the solution through a 0.45 μm membrane filter. Filtrate was preserved with 6 N $HNO_3$ and stored at 4 °C for arsenate analysis.

To investigate the pH impact on arsenate adsorption, 35 mL of 3 mg/L arsenate solution was mixed with 100 mg of Fe-GAC in a

series of 40-mL vials. The pH was adjusted to 2–12 initially using 0.1 N HCl or 0.1 N NaOH. During the adsorption period of 48 h, the pH of samples was readjusted to the targeted value using 0.1 N HCl or 0.1 N NaOH at 6, 12, 24, and 36 h. Fe-GAC was separated using a 0.45 μm membrane filter. Filtrate was preserved with 6 N $HNO_3$ and stored at 4 °C for arsenate analysis.

### 2.6. Analytical methods

Arsenate analysis was conducted via a Spectro Genesis Inductively Coupled Plasma-Optical Emission Spectroscopy (ICP-OES) at 189.042 nm in accordance with the USEPA method 200.5. A calibration curve, with a concentration series of 0, 0.05, 0.1, 0.4, 1.0, and 5.0 mg/L, was prepared using an arsenic standard solution (1000 μg/mL in 2% nitric acid, Ultra Scientific certified). The correlation coefficient ($R^2$) was always higher than 0.999. This method had an arsenic detection limit of 30 μg/L. For the analytical quality control, an instrument performance check solution (0.5 mg/L) was analyzed after every 10 samples. A 10% variation would halt the analysis and the ICP was programmed to recalibrate the arsenic analytical method. Spiked experimental blank/samples were adopted as quality control measures and the recovery rate was between 95% and 104%. Calibration blank was placed after high-concentration samples to minimize the carry-over effect.

The iron concentration in adsorption tests was analyzed simultaneously by the ICP-OES to monitor the stability of impregnated iron. Although iron and arsenic interfere with each other in ICP analysis, because the iron concentration was found very small (<0.3 mg/L) in all isotherm tests, the interference caused by iron at 189.042 nm was negligible.

## 3. Results and discussion

### 3.1. Preparation of Fe-GAC

It is difficult to achieve high amounts, even distribution, and stability for impregnated iron inside GAC in one step. This new synthesizing method is a multi-step procedure in which a small amount of iron is impregnated in GAC to achieve full penetration and even distribution in each step. Then, by repeating this process, high amounts of iron can be achieved as well as an even iron distribution inside GAC. Ferrous was used as the precursor because it is soluble at a wide range of pH and can diffuse deep into the internal pores of GAC [23]. However, ferrous impregnated in GAC may not be stable because it can re-dissolve into solution. Therefore, in the synthesis process, the drying step was purposely extended to 10 h to stabilize iron inside GAC by the conversion of ferrous to ferric using oxygen in air in the convective oven. In this step, most ferrous chloride is expected to be oxidized to ferric chloride, ferric oxide, and ferric hydroxide.

Two GACs, Darco 20 × 50 and Norit RX3 EXTRA, were used for iron impregnation to examine the capability of this synthesizing method. As shown in Fig. 1, iron contents were 2.03% for Darco 20 × 50 and 0.77% for Norit RX3 EXTRA after the first 24 h treatment. Iron contents increased almost linearly with repetitions, 1.03% per repetition for Darco 20 × 50 and 0.74% per repetition for Norit RX3 EXTRA. If all pores of GAC are assumed to be filled with 0.5 M ferrous solution ideally in each repetition, according to the total pore volumes of GACs shown in Table 1, the impregnated iron is 26.6 mg/g for Darco 20 × 50 and 19.4 mg/g for Norit RX3 EXTRA per repetition. Therefore, the ideal increment of iron content in each repetition will be 2.60% for Darco 20 × 50 and 1.90% for Norit RX3 EXTRA. The experimental value of iron increment per repetition is about 40% of calculated values for both GACs. Most likely some of impregnated iron re-dissolved into the liquid phase in the following repetitions

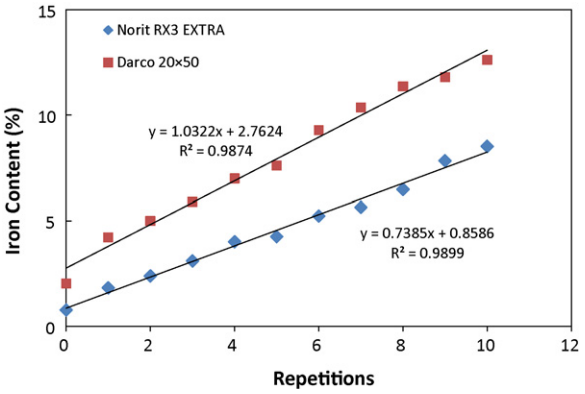


**Fig. 1.** Increment of impregnated iron content in the synthesizing process.

to cause the difference between experimental values and calculated values. This synthesizing method is easy to conduct and the iron content can simply be controlled by the number of repetitions. After 10 repetitions, 12.62% and 8.52% iron were impregnated in Darco 20 × 50 and Norit RX3 EXTRA, respectively. More iron may be impregnated with more repetitions.

### 3.2. Stability of impregnated iron

Iron desorption tests were carried out firstly to examine the stability of impregnated iron and results indicated that without post-treatment some of impregnated iron was unstable. Depending on iron content of Fe-GACs, 6–46% of impregnated iron were lost in desorption tests. EDS analysis revealed that large amounts of chlorine in Fe-GACs (Fig. S1a, supporting information), which implied the existence of ferric or ferrous chlorides. Ferric and ferrous chlorides may dissolve into solution because ferric chloride and ferrous chloride have solubility of 92 g/100 mL and 68.5 g/100 mL in water at 20 °C, respectively. A post-treatment described in Section 2.2 was designed to further stabilize impregnated iron through conversion of iron chlorides to ferric hydroxide which is sparingly soluble (Table S1). After post-treatment, desorption tests were conducted again and results showed that the post-treatment successfully stabilized iron in Fe-GACs. EDS analysis, conducted on post-treated Fe-GACs, indicated that the amounts of chlorine reduced significantly (Fig. S1b). The stability of impregnated iron was also tested on Fe-GAC with 4.22% iron in the adsorption test with pH variation of 2–11. As shown in Fig. 2, impregnated iron dissolved when pH was below 4. At pH 2.08, dissolved iron concentration was 25 mg/L, which is equivalent to 21% of impregnated iron. Impregnated iron was very stable when pH was above 4. Because pH is usually neutral in water resources, no concern is necessary for the iron stability

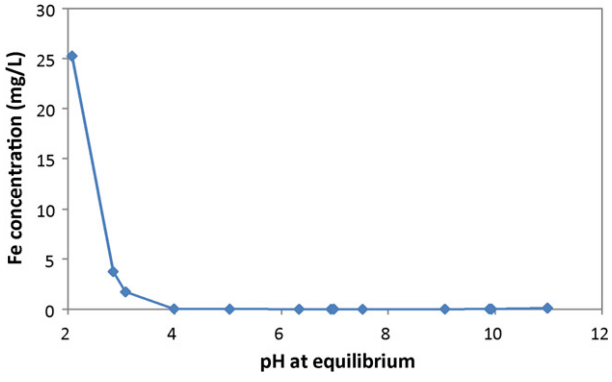


**Fig. 2.** Stability of impregnated iron on Darco 20 × 50 Fe-GAC with 4.22% iron.

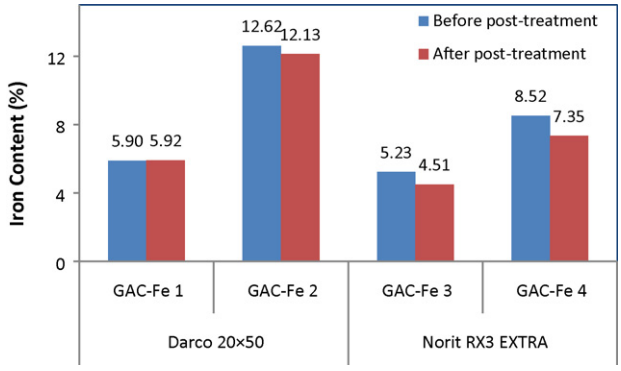


**Fig. 3.** Iron content before and after post-treatment.

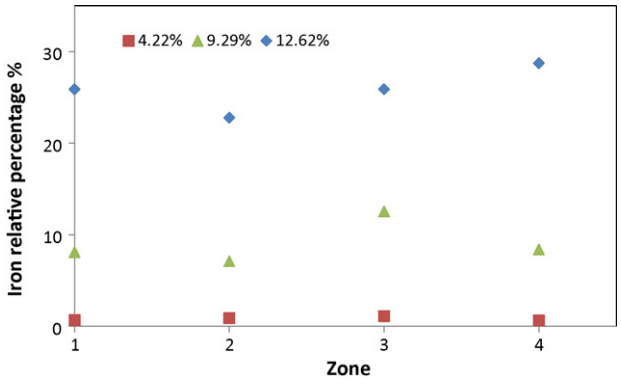


**Fig. 4.** Iron distribution on the cross-section of Darco 20 × 50 Fe-GACs.

of Fe-GACs. The iron stability was also monitored in all adsorption tests using ICP and the dissolution of impregnated iron was negligible.

The iron content of post-treated Fe-GACs was measured to investigate the loss of iron during the post-treatment process. Fig. 3 shows that the iron loss in the post-treatment was insignificant.

### 3.3. Characterization of Fe-GAC

#### 3.3.1. Distribution of impregnated iron

Darco 20 × 50 Fe-GACs, with iron contents of 4.22%, 9.29% and 12.62%, were analyzed using SEM/EDS to investigate the iron distribution inside GAC. Fig. 4 shows the relative weight percentages of iron in the four zones from the edge to the center on the cross-section of Fe-GACs (Fig. S2), which indicated that iron was evenly distributed on the cross-section of GACs rather than concentrated on the edge. The variation of the iron relative weight percentages across the cross-section of Fe-GAC is likely caused by the heterogeneity of pore sizes and morphologies of GAC itself. The even iron distribution was found in Norit RX3 EXTRA Fe-GAC with iron content of 8.52% as well.

As shown in Fig. 4, relative weight percentages of iron are different between SEM/EDS analysis and the results from acid extraction method described in Section 2.3.1. With the acid extraction method as reference, SEM/EDS analysis generated underestimate at low iron content (4.22%), overestimate at high iron content (12.62%), and matched estimate with medium iron content (9.22%). EDS detects elements on the surface of samples with selected penetration depth. For Fe-GAC with low iron content, it is expected that iron distributed evenly on GAC internal surfaces in both macro-pores and micro-pores. Because most internal surface areas are contained in micro-pores and crosscutting of the Fe-GAC samples will not expose most micro-pores, EDS is not able to detect unexposed iron in micro-pores and resulted in underestimated iron contents. At high iron contents, iron crystals or nano-scale iron deposits may form (see discussion in Section 3.3.2) in macro-pores. Exposure of large amount of iron in macro-pores could be the reason for overestimation of iron content from EDS analysis.

In addition to EDS analysis, mapping of iron distribution on the cross-section of Darco 20 × 50 Fe-GAC with 9.29% iron shows that impregnated iron covered the entire cross-section of Fe-GAC and higher iron content was observed in the macro-pores (cracks) of Fe-GAC (Fig. S3).

#### 3.3.2. Morphology of impregnated iron

Internal structure and morphology of Norit RX3 EXTRA Fe-GAC with 8.52% iron are shown in Fig. 5. Iron formed rod-shape nano-size particles in macro-pores of GAC. In Fig. 5b, iron rods were measured approximately 300 nm in length and 40 nm in diameter. Areas without iron rods in Fig. 5a are believed to be areas with micro- and meso-pores which can be seen from lower left part of Fig. 5b. Due to the constraint of pore size, impregnated iron cannot form rod-shape nano-particles in these areas; however, iron is believed to exist in a smaller scale. Fig. 6 shows morphologies of virgin and iron impregnated Darco 20 × 50 GAC. Instead of rod-shape nano-particles, irregular shapes of iron deposited in Darco 20 × 50 Fe-GAC with low iron content (Fig. 6b and c) while nano-iron crystals were observed in Fe-GAC with high iron content (Fig. 6d). The heterogeneity of pores and surface morphologies of GAC Darco 20 × 50 can be seen in Fig. 6.

#### 3.3.3. Iron species

Both post-treated and non-post-treated Fe-GACs were pulverized for XRD analyses to identify iron species. The major peaks of processed XRD spectra (Fig. 7) matched well with the crystalline iron species akaganeite (β-FeOOH); while, the raw XRD spectrum (Fig. S4) implies that significant amounts of amorphous iron existed in Fe-GAC as well. The species of impregnated iron are affected by impregnation methods and synthesizing conditions [26,30]. Jang et al. [26] reported that impregnated iron formed akaganeite at syn-

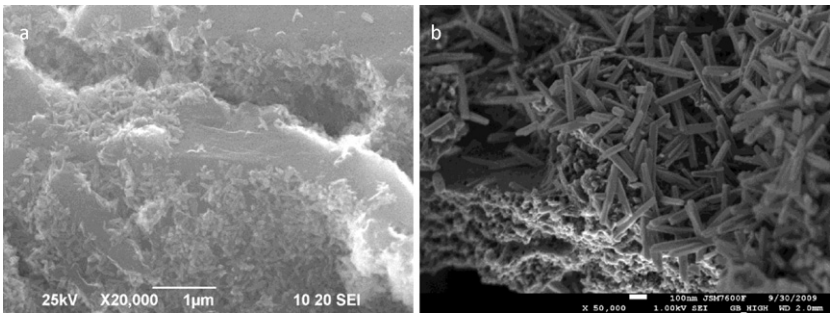


**Fig. 5.** SEM images of Norit RX3 EXTRA Fe-GAC with 8.52% iron.

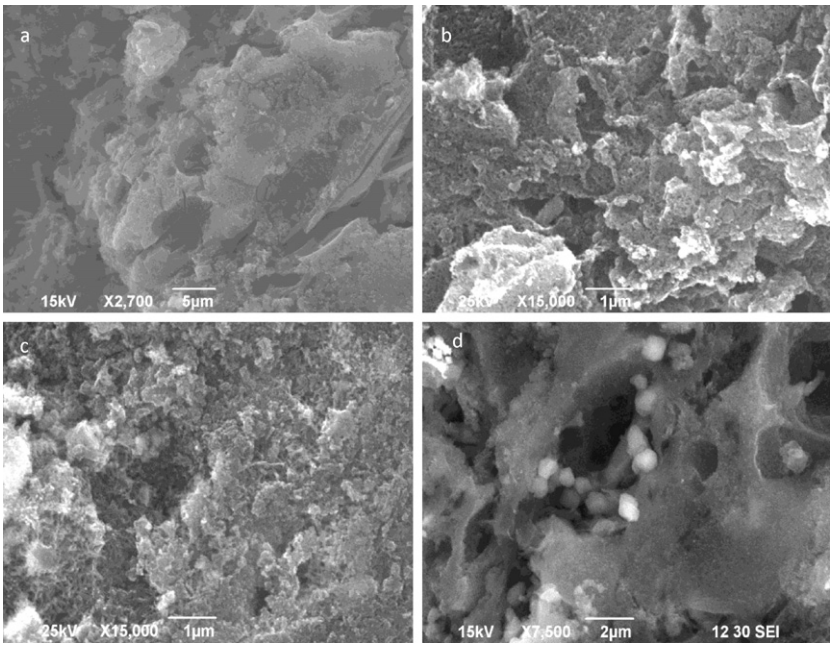


**Fig. 6.** SEM images of Darco 20 × 50 Fe-GACs (a: virgin GAC; b: 4.22%; c: 9.29%; and d: 12.62% iron).

thesizing temperature 80 °C and amorphous hydrous ferric oxide (HFO) at 60 °C. However, Gu et al. [23] found that impregnated iron in GAC, synthesized at 80 °C, were all in amorphous state. Results of this study found that impregnated iron existed as both crystalline and amorphous species in GAC.

### 3.4. pH impact on arsenic adsorption

pH is one of the most important factors affecting arsenate adsorption in the liquid phase [21–23,26,27], because the arsenate species and the surface charge of Fe-GACs in liquid phase depend on pH. The impact of pH on arsenate removal was studied with pH values ranging from 2 to 11 using 100 mg Darco 20 × 50 Fe-GAC with 4.22% iron and 35 mL 3 mg/L arsenate solution. As shown in Fig. 8, arsenic removal rate maintained close to 100% at pH 2–6 and declined slightly at pH 6.0–7.0. When pH was above 7.0, arsenic removal rate declined quickly. To minimize the impact of pH variation on isotherm tests as well as to keep experimental conditions close to natural waters, the pH in arsenate isotherm tests was controlled at 7.0 using bicarbonate buffer solution.

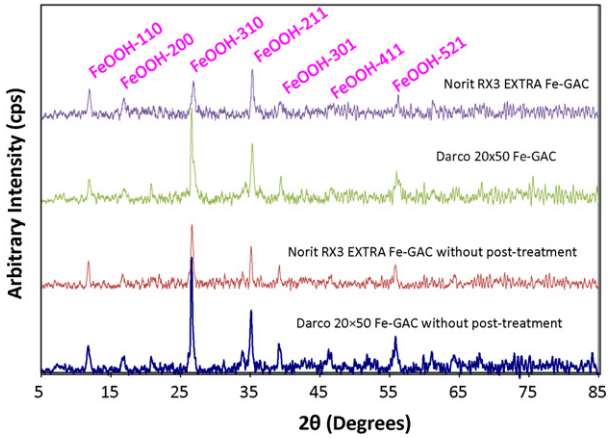


**Fig. 7.** XRD spectra of Fe-GACs.

To evaluate the impact of pH on arsenate adsorption, major arsenate species in different pH ranges are included in Fig. 8. Arsenate species in aqueous phase exist mainly as $H_3AsO_4$ at pH less than 2.2 ($pK_1$), $H_2AsO_4^-$ at pH between 2.2 and 6.98 ($pK_2$), $HAsO_4^{-2}$ at pH between 6.98 and 11.5 ($pK_3$), and $AsO_4^{-3}$ at pH above 11.5. $pH_{zpc}$ is the pH at which adsorbents have a net zero surface charge [38,39]. The $pH_{zpc}$ for Fe-GAC was between 8.2 and 8.7 [21]. As shown in Fig. 8, Fe-GACs becomes more positively charged when pH is less than 8.3 ($pH_{zpc}$) and more negatively charged when pH is above 8.3. As pH increased, the attractive force between Fe-GAC and arsenate became less and changed to repulsive force when pH above 8.3. The change of the electrostatic force between arsenate species and Fe-GAC explained the pH impact on arsenate adsorption.

### 3.5. Arsenate adsorption on Fe-GAC

Darco 20 × 50 Fe-GACs with five different iron contents were used in arsenate adsorption tests to determine the adsorption capacities. As shown in Fig. 9, virgin GAC has little arsenate adsorption capacity while impregnated iron enhanced the adsorption capacity considerably. The Langmuir model (Eq. (2)) was used to interpret the arsenate adsorption on Fe-GACs because arsenic

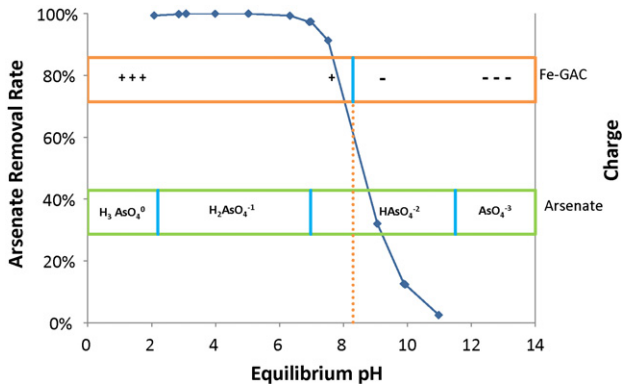


**Fig. 8.** Impact of pH on the arsenic adsorption on Darco 20 × 50 Fe-GAC with 4.22% iron.

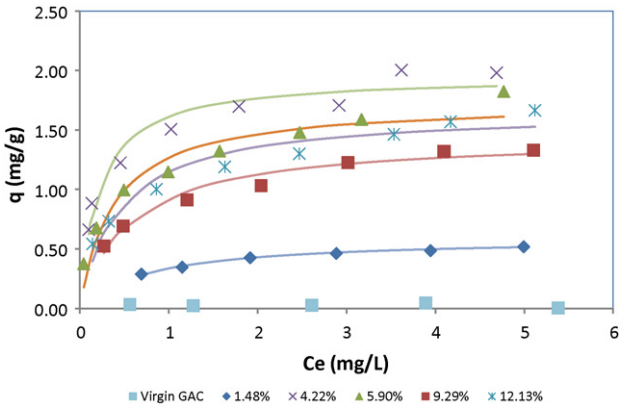


**Fig. 9.** Arsenate isotherm curves for Darco 20 × 50 Fe-GACs (lines are the Langmuir model fits).

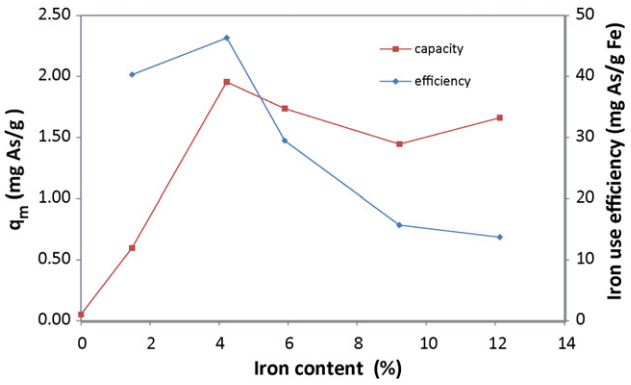


**Fig. 10.** Relationship between iron content and arsenate adsorption capacity/iron use efficiency.

adsorption on iron is site-specific chemisorption [39]. Inverted Langmuir model (Eq. (3)) is commonly used for parameter estimation via linear regression. However, this transformation introduces serious bias to the estimated parameters, and especially when isotherm tests covered a wide range of equilibrium concentration. Because the transformation assigns heavier weight to the points with low equilibrium concentration and lighter weight to the points with high concentration. In this study, nonlinear regressions were conducted using Statistical Analysis System (SAS) to obtain nonbiased estimates of Langmuir parameters. (Fig. S5 shows the improvement of nonlinear regression from linear regression on arsenate adsorption using Darco 20 × 50 Fe-GAC with 5.90% iron.)

As shown in Fig. 9 and Table 2, Langmuir model fits arsenate adsorption isotherm curves very well with $R^2$ between 0.93 and 0.99. In adsorption tests, pH was controlled in a narrow range of 6.90 ± 0.1, which minimized the pH impact on adsorption capacities to better demonstrate the impact of iron contents. Equilibrium arsenate concentrations were controlled at 0.05–5 mg/L, which enabled a better comparison of maximum adsorption capacity in the Langmuir model because isotherm parameters depend on the equilibrium concentration range [40]. The maximum adsorption capacity varied between 0.6 mg/g and 1.95 mg/g for Fe-GACs with iron contents from 1.48% to 12.13%. The value of parameter $b$ varied between 1.3 L/mg and 4.7 L/mg with an average of 2.54 L/mg, which is much higher than values reported in literature [23,24,29]. The parameter $b$ in Langmuir model is related primarily to the net enthalpy of adsorption that reflects the strength of binding of the adsorbate to the adsorbent, or simply as the affinity of the adsorbent for the adsorbate [38,41]. Higher affinity of Fe-GACs for arsenic means that most of the adsorption capacities of Fe-GACs can be realized at low arsenic concentration (Fig. S6), which is very common in water treatment processes [2].

$$q = q_m \frac{bc_e}{1 + bc_e} \tag{2}$$

$$\frac{1}{q} = \frac{1}{q_m b} \cdot \frac{1}{c_e} + \frac{1}{q_m} \tag{3}$$

It was also found that Fe-GACs without post-treatment exhibited higher maximum adsorption capacity and affinity in this study. Darco 20 × 50 Fe-GAC (5.90%) without post-treatment exhibited significantly higher "adsorption" capacity ($q_m$ = 8.48 mg/g) and "affinity" ($b$ = 22.6 L/mg) than the one with post-treatment (Fig. S7 and Table S2). Unstable iron dissolved into solution and removed arsenic in liquid phase rather than adsorption in solid phase. This may not be favored in water treatment process because dissolved iron bonded with arsenic may exist in solution as colloid particles. Unstable iron may also cause secondary water quality concern. Therefore, it is crucial to stabilize impregnated iron inside GAC.

### 3.6. Impact of iron content on arsenate adsorption capacity and iron use efficiency

Impact of the amount of impregnated iron on arsenic adsorption capacity has not been systematically evaluated in literature. Thus, in this study, arsenate isotherm tests were conducted on a series of Fe-GACs with different iron contents to systematically investigate the relationship between iron content and arsenate adsorption capacity. The relationships between the iron content and maximum adsorption capacity ($q_m$) and iron use efficiency (defined as $q_m$ divided by total amount of impreganted iron) were evaluated. As shown in Fig. 10, arsenate adsorption capacity increased as more iron was impregnated and reached a peak capacity of 1.95 mg/g when iron content increased to 4.22%. Further increase of iron content resulted in capacity decreasing gradually. Similar results were observed by Gu et al. [23] that arsenate removal rate peaked at Fe-GAC with iron content of 2.34%.

Iron use efficiency is used to explain the mass of arsenate (mg) may be adsorbed on a unit mass (g) of impregnated iron. When iron content is less than 4.22%, iron use efficiency maintained at a high level, from 40 mg As/g Fe to 46 mg As/g Fe. Then, it dropped rapidly to 14 mg As/g Fe as iron content increased to 12.13%. Arsen-

**Table 2**
The parameters in Langmuir model estimated by nonlinear regression.

| Iron content (%) | pH | $c_e$ (mg/L) | $q_m$ (mg/g) | $b$ (L/mg) | $R^2$ |
|---|---|---|---|---|---|
| Virgin GAC | 6.80 ± 0.05 | 0.56–5.38 | –[a] | – | – |
| 1.48 | 6.96 ± 0.17 | 0.69–4.99 | 0.60 | 1.3 | 0.9934 |
| 4.22 | 6.99 ± 0.05 | 0.01–4.69 | 1.95 | 4.7 | 0.9448 |
| 5.90 | 6.99 ± 0.06 | 0.04–4.77 | 1.74 | 2.7 | 0.9309 |
| 9.29 | 6.81 ± 0.03 | 0.27–5.11 | 1.44 | 1.8 | 0.9627 |
| 12.13 | 6.81 ± 0.03 | 0.14–5.12 | 1.66 | 2.2 | 0.9303 |

[a] Isotherm curve of virgin GAC was not interpreted by Langmuir model.

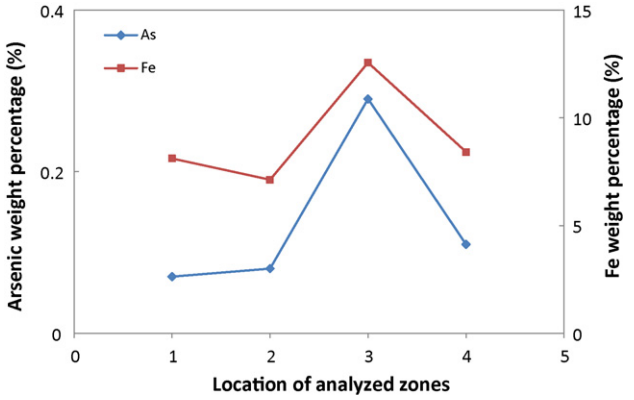


**Fig. 11.** Adsorbed arsenate distribution in Darco 20 × 50 Fe-GAC with 9.29% iron.

ate adsorption on iron is a site-specific surface reaction. Therefore, the total surface area of impregnated iron (adsorptive sites) determines the maximum adsorption capacity and the specific surface area of impregnated iron (adsorptive sites density) determines the iron use efficiency, while the surface characteristics of impregnated iron determine the affinity for arsenate. When only a small amount of iron is impregnated in GAC, the iron is expected to distribute in a single layer on the internal surface of GAC. Therefore, the iron possesses a large specific surface area that reflects as high iron use efficiency. Due to the small amount, however, the adsorption capacity remains relative low. As more iron is impregnated in GAC, more surface area of GAC is covered by iron. Adsorption capacity increases and iron use efficiency remains at a high level. When the amounts of iron keep increasing, impregnated iron starts forming multi-layer. As multi-layers and nano-scale iron particles formed, which was observed in SEM analysis, mass of impregnated iron increased faster than the increasing of its surface area. High amounts of iron may cause blockages in GAC pores as well, resulting in declining of the specific surface area. As reflected in arsenic adsorption, both adsorption capacity and iron use efficiency decrease with more impregnated iron.

### 3.7. Distribution of absorbed arsenate in Fe-GAC

For porous adsorbents, the internal surface area contributes major part of adsorption capacity [42]. To date, it is still not clear whether arsenic can diffuse deep into to the core of Fe-GAC [23,27]. EDS analyses were conducted on spent Fe-GACs to evaluate the distribution of the adsorbed arsenate from the edge to the center on the cross-section of Fe-GACs. Adsorbed arsenate penetrated into the center of Fe-GAC and the amounts of adsorbed arsenate followed the amounts of impregnated iron exactly (Fig. 11). The ratios of arsenate to iron, calculated based on the relative weight percentages, varied from 0.009 to 0.023 with an average of 0.014, which is consistent with the value 0.0155 (by weight) that was calculated from arsenate adsorption tests.

## 4. Conclusions

A new multi-step procedure was developed to impregnate GAC with high amounts of iron for arsenic removal from drinking water. Fe-GACs were evaluated based on four parameters: amount of impregnated iron, distribution of impregnated iron, iron stability, and arsenate adsorption capacity.

1. Impregnated iron, as high as 12.62%, was evenly and stably distributed inside GAC using the multi-step synthesizing method.
2. Impregnated iron formed rod-shape nano-size particles in Norit RX3 EXTRA Fe-GAC and nano-size crystal in Darco 20 × 50 Fe-GAC. Crystalline (akaganeite) and amorphous iron species co-existed in Fe-GACs.
3. Isotherm data of arsenate adsorption tests were successfully interpreted by the Langmuir model. The maximum arsenate adsorption capacity of Fe-GACs increased quickly to1.95 mg/g when iron content increased to 4.22%, while it decreased with more impregnated iron (>4.22%).
4. The iron use efficiency maintained at a high level (40–46 mg As/g Fe) when iron content was less than 4.22%; it then decreased to 14 mg As/g Fe when iron content increased to 12.13%.
5. Fe-GACs in this study exhibited high affinity (1.3–4.7 L/mg) for arsenate.
6. Fe-GACs performed better at the acidic condition than the basic condition on arsenate adsorption; specifically, the arsenate removal rate maintained close to 100% with pH less than 6 and declined quickly with pH above 7.
7. Adsorbed arsenate penetrated into the center of Fe-GACs and exactly followed the distribution of impregnated iron.

## Acknowledgements

The fellowship from North Dakota Water Resources and Research Institute (NDWRRI) and USGS are gratefully appreciated. The authors thank Curt Doetkott and Li Cao at the Statistical Consulting Office at North Dakota State University for their helps on statistical analyses. The authors also thank American Norit Co. Inc. for generously providing GAC samples to support this research.

## Appendix A. Supplementary data

Supplementary data associated with this article can be found, in the online version, at doi:10.1016/j.jhazmat.2010.08.066.

## References

[1] C. Jain, I. Ali, Arsenic: occurrence, toxicity and speciation techniques, Water Res. 34 (2000) 4304–4312.
[2] P.L. Smedley, D.G. Kinniburgh, A review of the source, behaviour and distribution of arsenic in natural waters, Appl. Geochem. 17 (2002) 517–568.
[3] M.J. DeMarco, A.K. SenGupta, J.E. Greenleaf, Arsenic removal using a polymeric/inorganic hybrid sorbent, Water Res. 37 (2003) 164–176.
[4] CSME, Geology and Geochemistry of Arsenic Occurrences in Groundwater of Six Districts of West Bengal, Report of the Centre for Study of Man and Environment, Calcutta, 1997.
[5] DPHE/BGS/MML, Groundwater Studies for Arsenic Contamination in Bangladesh. Phase I: Rapid Investigation Phase. BGS/MML Technical Report to Department for International Development, UK, vol. 6, 1999.
[6] G.F. Sun, G.J. Dai, F.J. Li, H. Yamauchi, T. Yoshida, H. Aikawa, The present situation of chronic arsenism and research in China, in: W.R. Chappell, C.O. Abernathy, R.L. Calderon (Eds.), Arsenic Exposure and Health Effects, Elsevier, Amsterdam, 1999, pp. 123–126.
[7] M. Berg, H.C. Tran, T.C. Nguyen, H.V. Pham, R. Schertenleib, W. Giger, Arsenic contamination of groundwater and drinking water in Vietnam: a human health threat, Environ. Sci. Technol. 35 (2001) 2621–2626.
[8] USEPA, National Primary Drinking-Water Regulations: Arsenic and Clarifications to Compliance and New Source Contaminants Monitoring; Final Rule: Federal Register, U.S. Code of Federal Regulations, vol. 66, 2001, pp. 6976–7066.
[9] E.O. Kartinen, C.J. Martin Jr., An overview of arsenic removal processes, Desalination 103 (1995) 78–88.
[10] USEPA, Arsenic Treatment Technologies for Soil, Waste, and Water, EPA-542-R-02-004, 2002.
[11] D.L. Boccelli, M.J. Small, D.A. Dzombak, Enhanced coagulation for satisfying the arsenic maximum contaminant level under variable and uncertain conditions, Environ. Sci. Technol. 39 (2005) 6501–6507.
[12] A.M. Sancha, Review of coagulation technology for removal of arsenic: case of Chile, J. Health Popul. Nutr. 24 (2006) 267–272.
[13] D.A. Clifford, G.L. Ghurye, A.R. Tripp, As removal using ion exchange with spent brine recycling, J. Am. Water Works Assoc. 95 (2003) 119–130.
[14] X.Z. Zhang, K. Jiang, Z.B. Tian, W.Q. Zhang, Removal of arsenic in water by an ion-exchange fiber with amino groups, J. Appl. Polym. Sci. 110 (2008) 3934–3940.

[15] H.R. Lohokare, M.R. Muthu, G.P. Agarwal, U.K. Kharul, Effective arsenic removal using polyacrylonitrile-based ultrafiltration (UF) membrane, J. Membr. Sci. 320 (2008) 159–166.
[16] B. Buche, L. Owens, Removal of arsenic from ground water using granular activated, J. Am. Water Works Assoc. (1996).
[17] G.N. Manju, M.C. Gigi, T.S. Anirudhan, Evaluation of coconut husk carbon for the removal of arsenic from water, Water Res. 32 (1998) 3062–3070.
[18] W. Zhang, Q.G. Chang, W.D. Liu, B.J. Li, W.X. Jiang, L.J. Fu, Selecting activated carbon for water and wastewater treatability studies, Environ. Prog. 26 (2007) 289–298.
[19] C.P. Huang, L. Vane, Enhancing $As^{5+}$ removal by $Fe^{2+}$ treated activated carbon, J. Water Pollut. Contr. Fed. 61 (1989) 1596–1603.
[20] M. Pakula, S. Biniak, A. Swiatkowski, Chemical and electrochemical studies of interactions between iron(III) ions and an activated carbon surface, Langmuir 14 (1998) 3082–3089.
[21] B. Reed, R. Vaughan, L.Q. Jiang, As(III), As(V), Hg, and Pb removal by Fe-oxide impregnated activated carbon, J. Environ. Eng. 126 (2000) 869–873.
[22] K. Payne, T. Abdel-Fattah, Adsorption of arsenate and arsenite by iron-treated activated carbon and zeolites: effects of pH, temperature, and ionic strength, J. Environ. Sci. Health A 40 (2005) 723–749.
[23] Z.M. Gu, J. Fang, B.L. Deng, Preparation, Evaluation of GAC-based iron-containing adsorbents for arsenic removal, Environ. Sci. Technol. 39 (2005) 3833–3843.
[24] W.F. Chen, R. Parette, J. Zou, F.S. Cannon, Arsenic removal by iron-modified activated carbon, Water Res. 41 (2007) 1851–1858.
[25] D. Mohan, C. Pittman Jr., Arsenic removal from water/wastewater using adsorbents – a critical review, J. Hazard. Mater. 142 (2007) 1–53.
[26] M. Jang, W.F. Chen, F.S. Cannon, Preloading hydrous ferric oxide into granular activated carbon for arsenic removal, Environ. Sci. Technol. 42 (2008) 3369–3374.
[27] K.D. Hristovski, P.K. Westerhoff, T. Moller, P. Sylverster, Effect of synthesis conditions on nano-iron (hydro)oxide impregnated granular activated carbon, Chem. Eng. J. 146 (2009) 237–243.
[28] G. Muñiz, V. Fierro, A. Celzard, G. Furdin, G. Gonzalez-Sánchez, M.L. Ballinas, Synthesis, characterization and performance in arsenic removal of iron-doped activated carbons prepared by impregnation with Fe(III) and Fe(II), J. Hazard. Mater. 165 (2009) 893–902.
[29] Q. Zhang, Y. Lin, X. Chen, N. Gao, A method for preparing ferric activated carbon composites adsorbents to remove arsenic from drinking water, J. Hazard. Mater. 148 (2007) 671–678.
[30] O. Thirunavukkarasu, T. Viraraghavan, K. Subrama, Arsenic removal from drinking water using iron oxide-coated sand, Water Air Soil Pollut. 142 (2003) 95–1114.
[31] B.A. Manning, M. Hunt, C. Amrhein, J.A. Yarmoff, Arsenic(III) andarsenic(V) reactions with zerovalent iron corrosion products, Environ. Sci. Technol. 36 (2002) 5455–5461.
[32] S. Goldberg, C. Johnston, Mechanisms of arsenic adsorption on amorphous oxides evaluated using macroscopic measurements, vibrational spectroscopy, and surface complexation modeling, J. Colloid Interface Sci. 234 (2001) 204–216.
[33] D.M. Sherman, S.R. Randall, Surface complexation of arsenic(V) to iron(III) (hydr)oxides: structural mechanism from ab initio molecular geometries and EXAFS spectroscopy, Geochim. Cosmochim. Acta 67 (2003) 4223–4230.
[34] S. Kanel, B. Manning, L. Charlet, H. Choi, Removal of arsenic(III) from groundwater by nanoscale zero-valent iron, Environ. Sci. Technol. 39 (2005) 1291–1298.
[35] R.J. Vaughan, B. Reed, Modeling As(V) removal by a iron oxide impregnated activated carbon using the surface complexation approach, Water Res. 6 (2005) 1005–1014.
[36] C. Xu, A. Teja, Supercritical water synthesis and deposition of iron oxide ($\alpha$-$Fe_2O_3$) nanoparticles in activated carbon, J. Supercrit. Fluids 39 (2006) 135–141.
[37] J. Liu, Comparative study on determination of iron contents in activated carbon, Linchan Huaxue Yu Gongye 15 (1995) 57–61.
[38] W.J. Weber Jr., A.D. Francis, Process Dynamics in Environmental Systems, John Wiley and Sons, Inc., New York, 1996.
[39] D.A. Dzombak, F.M.M. Morel, Surface Complexation Modeling: Hydrous Ferric Oxide, Wiley, New York, 1990.
[40] H. Sontheimer, J.C. Crittenden, R.S. Summers, Activated Carbon for Water Treatment, 2nd ed., DVGW-Forschungsstelle, Karlsruhe, Germany, 1988.
[41] M.M. Benjamin, Water Chemistry, McGraw-Hill, 2002.
[42] W.C. Ying, W. Zhang, Q.G. Chang, W.X. Jiang, G.H. Li, Improved methods for carbon adsorption studies for water and wastewater treatment, Environ. Prog. 25 (2006) 110–120.